AD-A049 780 WASHINGTON UNIV SEATTLE DEPT OF MECHANICAL ENGINEERING F/G 20/11
DYNAMIC PHOTOELASTIC AND DYNAMIC FINITE ELEMENT ANALYSES OF DYN--ETC(U)
JAN 78 S MALL, A S KOBAYASHI, Y URABE N00014-76-C-0060
UNCLASSIFIED TR-31 NL

| OF |
AD A049780

END
DATE FILMED
3-78
DDC

(12)

Office of Naval Research

(15) Contract N00014-76-C-0060 NR 064-478

(9) Interim Technical Report, No. (14) TR-1 31

(6) DYNAMIC PHOTOELASTIC AND DYNAMIC FINITE ELEMENT ANALYSES OF DYNAMIC TEAR TEST SPECIMENS.

(10) by
S. Mall, A.S. Kobayashi and Y. Urabe

(11) January 1978

(12) 27 p.

The research reported in this technical report was made possible through support extended to the Department of Mechanical Engineering, University of Washington, by the Office of Naval Research under Contract N00014-76-C-0060, NR 064-478. Reproduction in whole or in part is permitted for any purpose of the United States Government.

Department of Mechanical Engineering
College of Engineering
University of Washington

400 344

DYNAMIC PHOTOELASTIC AND DYNAMIC FINITE ELEMENT ANALYS S OF DYNAMIC TEAR TEST SPECIMENS

by

S. Mall, A.S. Kobayashi and Y. Urabe*
Department of Mechanical Engineering
University of Washington
Seattle, Washington 98195

ABSTRACT

Dynamic photoelasticity and dynamic finite element methods were used to study the transient response of dynamic tear test (DTT) specimen of a brittle material, Homalite-100. The dynamic stress intensity factors obtained from dynamic photoelasticity and dynamic finite element analysis were generally in excellent agreement with each other and showed that the NRL procedure of computing the dynamic fracture initiation toughness from strain gage measurements near the crack tip was reasonably accurate. Dynamic fracture toughness versus crack velocity relations were also obtained.

INTRODUCTION

In a previous paper [1], one of the authors used dynamic photoelasticity to analyze an enlarged photoelastic model of the dynamic tear test specimen (DTT) developed by the Naval Research Laboratories (NRL)[2,3,4]. This DTT specimen, which is a dynamically loaded three-point bend specimen, developed full thickness cleavage fracture without sidegrooving and is an ASTM proposed fracture specimen for assessing potential brittle fracture characteristics of ductile materials. Brittle fracture of the NRL type DTT specimen in the previous dynamic photoelasticity investigation was modeled by 356x88.9 mm specimens machined from 9.5 mm thick Homalite-100 plates subjected to an impact loading of 1.83 to 3.62 N-m

* Currently on leave from Takasago Technical Institute, Mitsubishi Heavy Industries, Takasago, Japan.

and led to the following four conclusions:

1. Fracture initiated after the first buildup of impact force in the hammer tip.
2. Dynamic fracture toughness, K_{ID}, decreases after reaching a maximum value as the crack propagated towards the impact site.
3. Dynamic tear energy which was computed from the measured dynamic fracture toughness varied with the sharpness of the starter crack.
4. The average dynamic energy release rate, $\mathcal{G}_{ID}$, was approximately equal to the critical strain energy release rate, $\mathcal{G}_{IC}$, of the Homalite-100 plate.

In a subsequent reevaluation of this DTT test result [5], dynamic fracture initiation toughness, K_{Id}, was estimated to be approximately equal to the static fracture toughness, K_{Ic}, in contradiction with the generally expected decrease in K_{Id} under impact loading. Such possible decrease in K_{Id} for the strain rate-sensitive Homalite-100 plates was conjectured from the observed trend in ductile metals with lesser strain rate sensitivity than Homalite-100 plates.

Results of the above dynamic photoelastic investigation presented some new concepts for the fracture dynamic response of DTT specimens as well as identified areas in which further investigation is necessary to clarify points of controversy. As a result, in this study DTT specimens machined from Homalite-100 plates were reanalyzed by dynamic photoelasticity as well as by the newly developed dynamic finite element method. The numerical technique was also used to compute the dynamic strains adjacent to the crack tip prior to and immediately after the onset of crack propagation and the dynamic stress intensity factor at the onset of crack propagation, K_{Id}, was then estimated through Loss' static procedure [3]. In the following some details of the experimental and numerical approaches as well as typical results are given.

EXPERIMENTAL SETUP

The experimental program consisted of dynamic photoelastic analysis of Homalite-100 models of DTT specimens where the emphasis in this study was to record the dynamic photoelastic patterns before and after crack initiation in order to interpolate the fracture toughness for dynamic loading at the instant of crack propagation. The system used to obtain a history of fracture initiation in a DTT specimen consisted of: (i) Cranz-Schardin 16 spark-gap camera and associated polariscope [1], (ii) a drop weight testing machine, (iii) a load transducer on the hammer tup and (iv) a circuitry to trigger the series of events for recording the photoelastic patterns, the load-time history and reference timings of each spark-gap firing.

The drop weight testing machine consisted of a free-falling weight with an instrumented striker tup and a rigidly supported anvil that provided loading of a simple three-point loaded beam. The drop weight varied from 2.75 to 27.5 kg (6 to 60 lbs.). Sliding friction between the drop weight and guiderails was minimized by two Thompson Super-12 ball bushings installed in the drop weight housing. The drop distance of the striker tup was 146 cm (5.75 in) and the impact velocity was about 150 cm/second (60 in/second).

The most critical component in impact testing is the load transducer which measures the load history prior to and after fracture. Such load history is particularly important in providing the necessary time-dependent boundary conditions for subsequent numerical analysis. A load-time record, however, was difficult to obtain due to the electric noise generated by the spark-gaps [6]. A four-arm strain gage bridge was mounted on a thinner central portion of the tup as shown in Figure 1. In addition, this tup was insulated with a tight fitting steel cover to shield the strain gages from external noise. The strain gage bridge output versus applied load relation were obtained by statically

calibrating the tup in a testing machine.

Another crucial problem involved in the DTT test was the triggering of this 16-spark-gap light source such that the dynamic events before the after crack propagation could be recorded. Such triggering was accomplished by closing a circuit between the tup and a thin copper strip which was glued to the impact area of the specimen. Contact between the tup and the strip triggered a delay signal from a Tektronix 555 oscilloscope which in turn triggered the light source delay system. In addition, a crack wire consisting of silver paint in front of the crack was used to record the initiation of crack propagation.

DTT TEST SPECIMEN

Configuration of the Homalite-100 DTT specimen is shown in Figure 2, and was selected in accordance with the recommended ASTM standard for a 16 mm (5/8 in) thick DTT specimen with the exception that the Homalite-100 photoelastic specimen had a nominal thickness of 9.5 mm (3/8 in).

In the tests reported previously [1], an initial saw crack in the DTT specimen was chiseled with a sharp blade to simulate a natural starter crack. The same sawed and chiseled starter crack did not produce predictable crack initiation time, which was crucial in this study for pretriggering the dynamic polariscope prior to crack propagation. The sawed and chiseled crack was replaced with a fatigue crack which produced reproducible crack initiation time. Thus all photoelastic specimens were fatigue cracked at a low load corresponding to approximately 10 percent of the nominal fracture toughness.

Dynamic material calibration tests were carried out to determine the stress-fringe constant, modulus of elasticity and Poisson's ratio at various strain rates as well as the static fracture toughness. A split Hopkinson bar system [7] with test specimens of 9.5x9.5x254 mms or 9.5x9.5x381 mms were used.

Table 1 shows the results thus obtained.

The static fracture toughness of the Homalite-100 sheets were determined by standard ASTM E-399 compact tension specimens with initial fatigued crack length of approximately 19 mm. Static fracture toughness, K_{Ic}, shown in the table was obtained by the formula also shown in ASTM E-399 standards [8].

DYNAMIC FINITE ELEMENT ANALYSIS

The dynamic finite element analysis used in this investigation has been dsecribed in detail in Reference [9]. The finite element breakdown of the photoelastic DTT specimen used in this investigation is shown in Figure 1. Initially, 300 nodes and 294 elements were used but later the finite element breakdown was reduced to 169 nodes and 144 elements in order to conserve computer time. A state of plane strain was assumed in this analysis.

The recorded load-time history, which is the necessary time dependent boundary condition for this finite element analysis, was modeled as an average effective load transmitted to the specimen with a time phase difference of 10 microseconds to account for the time stress wave to propagate from the point of impact to the strain gage location on the tup.

RESULTS OF DYNAMIC PHOTOELASTIC EXPERIMENTS

A total of four dynamic photoelastic experiments were conducted. Figure 2 shows typical enlargements of two frames out of the 16 dynamic photoelastic patterns of one of the tests.

Figure 3 shows the dynamic stress intensity factor before and after crack initiation in the four DTT tests. The interpolated fracture initiation toughness under dynamic loading, K_{Id}, in these DTT test specimens were within $\pm$ 3 percent of the static fracture toughness, K_{Ic}, of 415 kPa$\sqrt{m}$ (378 psi$\sqrt{in}$). This

coincidence in dynamic fracture toughness, K_{Id}, at the onset of crack propagation and static fracture toughness, K_{Ic}, was predicted in Reference [5] through extrapolation of six DTT test results due to the lack of the first dynamic isochromatic fringes prior to crack propagation. Both extrapolated results of Reference [5] and the present results show that the duration of the impact loading before crack propagation was of the order of 150-200 microseconds.

Figure 3 also shows that the dynamic stress intensity factor during crack propagation, i.e. dynamic fracture toughness, K_{ID}, increased gradually as the crack ran through approximately sixty percent of the specimen width and then decreased to about fifty percent of K_{Ic} as the crack propagated into the static compression zone. Such low K_{ID} indicates that the minimum resistance to dynamic crack propagation, K_{Im}, is equal to or less than fifty percent of the fracture toughness. This continued decrease of the dynamic stress intensity factor in contrast with the monotonously increasing static stress intensity factor in a static three-point bend specimen [9] in the initially compressive zone of the DTT specimens was also observed in Reference [1].

Variation in crack velocity, c, along the specimen width is shown in Figure 4. The maximum crack velocity recorded was 317 m/sec (12,500 in/sec), or $c/c_1 = 0.12$, which was considerably lower than the previously recorded maximum velocity of 457 m/sec (18,000 in/sec), or $c/c_1 = 0.19$ for a sharp crack and 622 m/sec (24,500 in/sec) or $c/c_1 = 0.26$ for a blunt crack [1]. Crack velocities in the new series of four DTT specimens gradually decresed or remained practically constant up to seventy-five percent of the width of the specimen and then suddenly drop as the crack penetrated into the initially compressed zone. This variation of crack velocity along the width of the specimen agrees well with the dynamic fracture analysis of a beam under constant bending moment by Freund and Herrman [11].

Cracks in these DTT specimens curved as they approached the point of impact, indicating the pre-existing lower state of compressive stress which causes the crack to turn temporarily near the impact point. In particular, the crack in specimen No. S101176-H exhibited a prominent S-shape near the impact point. Similar results are reported in Reference [1] where a high velocity crack generated by an initially blunt crack* ran into the compression zone before the stress could redistribute itself in a high tension state expected from static equilibrium.

RESULTS OF DYNAMIC FINITE ELEMENT ANALYSIS

Two test Nos. S100976-1-H and S101176-H which contained photoelastic records of the initial stage of impact prior to crack propagation were selected for dynanic finite element analysis. Recorded tup load with time obtained from oscilloscope trace is shown in Figures 5 and 6 of test Nos. S100976-1-H and S101176-H, respectively, with two idealized load-time curves which were used in dynamic finite element analysis. Also shown in Figures 5 and 6 are the crack tip positions which were obtained from recorded photoelastic patterns and lite-mike timings, as functions of time. Crack initiation time was interpolated from this crack extension versus time relationship. In addition, dynamic photoelastic patterns of this test showed that the crack wire, which was located at the starter crack tip, did not break at the instant of crack propagation.

Figures 7 and 8 show the dynamic stress intensity factors, K_{ID}, obtained numerically and experimentally in test Nos. S100976-1-H and S101176-H. Reasonable agreements between experimental and numerical dynamic stress intensity factors were found. Importance of accurate modeling of the impact pulse is underlined in this numerical analysis where a better correlation between experimental and

---

* Crack initiated under high K_Q.

numerical stress intensity factors might have been obtained if the exact pulse shape of the load transmitted to the DTT specimen was available.

Figures 9 and 10 show the development of numerical dynamic finite element analysis from the start of impact to crack initiation in test Nos. S100976-1-H and S101176-H. The experimentally obtained dynamic stress intensity factor together with the dynamic stress intensity factor obtained from the computed dynamic strains at two locations in the crack tip by the method proposed by Loss [3] are also shown in Figures 9 and 10. Loss' procedure involves the determination of an equivalent static fracture load, which is transmitted to the three-point bend specimen from experimentally measured dynamic strain at a suitable location in the vicinity of the crack tip in an actual steel DTT specimen. The dynamic stress intensity factor, K_{Id}, is then determined from this equivalent static load using the expression for K_{Id} given in ASTM E-399 [8]. The procedure then is to find such proper strain gage location, which is independent of the strain rate, for determining the equivalent static fracture load. Figures 9 and 10 show that strain gage location B will yield K_{Id} by Loss' procedure [3] with reasonable accuracy.

DISCUSSION

The above dynamic finite element analysis provides a direct output of energies involved in the dynamic fracture process. Such energies can be used to assess the engineering significance of Charpy and Izod impact tests which relate the total external work to the dynamic fracture resistance of the specimen. Although this total external work has been used extensively for qualitatively assessing the static and dynamic fracture resistance of materials, no fundamental material property has been determined from such impact tests. In order to provide further insight into the energy absorption during such impact testing, computed external

work, total strain energy, total kinetic energy and fracture energy for the two DTT specimens Nos. S100976-1-H and S101176-H are plotted in Figures 11 and 12. These figures show that the kinetic energy and fracture energies constitute approximately 85% and 6%, respectively, of the external work done. The above energies were computed up to the time when the crack tip reached the last boundary element. The relatively large ratio of kinetic energy to the external work indicates that the use of external work in the DTT type of specimens as a measure of the fracture resistance may be of doubtful value.

Because of the considerable interest [12] in establishing a relation between the dynamic fracture toughness, K_{ID}, versus a crack velocity relationship, c, as a material property, these values are plotted in Figure 13 for the four Homalite-100 specimens tested. Also shown in this figure are the averaged K_{ID} versus c relationship obtained by T. Kobayashi et al at the University of Maryland as well as results obtained from previously conducted DTT analysis [1]. Considerable scatter in data obtained in the DTT tests is in contrast to the more cohesive data points obtained in non-impact specimens [12].

If an average dynamic fracture toughness versus crack velocity relationship of the familiar Γ shape is drawn through the experimental data point shown in Figure 13, such a plot will show that the minimum resistance to dynamic crack propagation, K_{Im}, will be considerably different from the K_{Im} established for other statically loaded specimens.

CONCLUSION

The dynamic response of dynamic tear test specimen of a brittle material has been investigated by the use of dynamic photoelasticity and dynamic finite element analysis and the following conclusions were obtained:

(1) In the dynamic photoelastic investigation, the crack initiation dynamic

fracture toughness, K_{Id}, was found to be approximately equal to the static fracture toughness of K_{Ic}.

(ii) The minimum dynamic fracture toughness, K_{Im}, was found to be substantially lower than the static fracture toughness, K_{Ic}.

(iii) Loss' procedure of estimating K_{Id} from measured dynamic strain gage results has been found to be effective in calculating K_{Id} of this brittle material.

ACKNOWLEDGEMENTS

The results of this investigation were obtained in a research contract funded by the Office of Naval Research under Contract N00014-76-C-0060 NR 064-478. The authors wish to acknowledge the support and encouragement of Dr. N.R. Perrone and Dr. N. Basdagas of ONR during this course of this investigation.

REFERENCES

A049687

1. Kobayashi, A.S. and Chan, C.F., "A Dynamic Photoelastic Analysis of Dynamic Tear Test Specimen", Exper. Mech., Vol. 16, No. 5, May 1976, pp. 176-181.

2. "Standard Method of Test for Plane-Strain Fracture Toughness of Metallic Materials, E399-74", Book of ASTM Standards, Part 31, ASTM, Philadelphia, Pennsylvania, 1974.

3. Loss, F.J., "Dynamic Fracture Toughenss of Reactor Pressure Vessel Steels", presented at the International Experts Meeting on Elastic-Plastic Fracture Mechanics, San Francisco, June 24-25, 1976.

4. Hawthorne, J.R. and Loss, F.J., "Fracture Toughness Characterizations of Shipbuilding Steel", Ship Structure Committee Report SCC-248, U.S. Coast Guard Headquarters, 1976.

5. Kobayashi, A.S. and Mall, S., "Dynamic Photoelastic Analysis of Three Fracture Specimens", Proc. of an International Conference on Dynamic Fracture Toughness, London, England, 5-7 July 1976, pp. 259-272.

6. Irwin, G.R., Dally, J.W., Kobayashi, T., Fourney, W.L. and Etheridge, J.M., "A Photoelastic Characterization of Dynamic Fracture", NUREC-0072, U.S. Nuclear Regulatory Commission, December 1976.

7. Bradley, W.B. and Kobayashi, A.S., "An Investigation of Propagating Cracks by Dynamic Photoelasticity", Experimental Mechanics, Vol. 10, No. 3, March 1970, pp. 106-113.

8. "Standard Method of Test for Plane-Strain Fracture Toughness of Metallic Materials, E 399-74", Book of ASTM Standards, Part 31, ASTM, Philadelphia, 1974.

9. Kobayashi, A.S., Mall, S., Urabe, Y. and Emery, A.F., "A Numerical Dynamic Fracture Analysis of Three Wedge-Loaded DCB Specimens", Proc. of the Int'l Conf. on Numerical Methods in Fracture Mechanics, University College of Swansea, Jan. 9-13, 1978.

10. Atluri, S.N., Kobayashi, A.S. and Nakagaki, M., "Application of an Assumed Displacement Hybrid Finite Element Procedure to Two-Dimensional Problems in Fracture Mechanics", AIAA Journal, Vol. 13, No. 6, 1975, pp. 734-739.

11. Freund, L.B. and Hermann, G., "Dynamic Fracture of a Beam or Plate in Bending", Journal of Applied Mechanics, Vol. 98, No. 1, March 1976, pp. 112-116.

12. Kobayashi, T. and Dally, J.W., "The Relation Between Crack Velocity and Stress Intensity Factor in Birefringent Polymers", Fast Fracture and Crack Arrest, ASTM STP 627, 1977, pp. 257-273.

TABLE 1

AVERAGE MECHANICAL AND OPTICAL PROPERTIES OF HOMALITE-100

E_S GPa (ksi)	3.72 (540)
E_D GPa (ksi)	4.80 (696)
ν_S	0.36
ν_D	0.36
f_{σ_S} MPa-mm/fringe (psi-in/fringe	21.5 (123)
f_{σ_D} MPa-mm/fringe (psi-in/fringe	20.7 (118)
ρ kg-sec^2/m^4 (lb-sec^2/in^4)	122 (0.000112)
c_1 m/sec (in/sec)	2590 (102,000)
c_2 m/sec (in/sec)	1210 (47,800)
c_p m/sec (in/sec)	2140 (84,400)
K_{Ic} kPa$\sqrt{m}$ (psi$\sqrt{in}$)	415 (378)

NOTE: (i) Subscript S is for static properties
Average strain rate was 1.8×10^{-3} strain/sec

(ii) Subscript D is for dynamic properties
Average strain rate was 60 strain/sec

(iii) E, ν, f_σ and ρ are modulus of elasticity, Poisson's ratio, material stress-optic coefficient and density, respectively.

(iv) c_1, c_2, and c_p are dilatational, distortional and plate wave velocity, respectively.

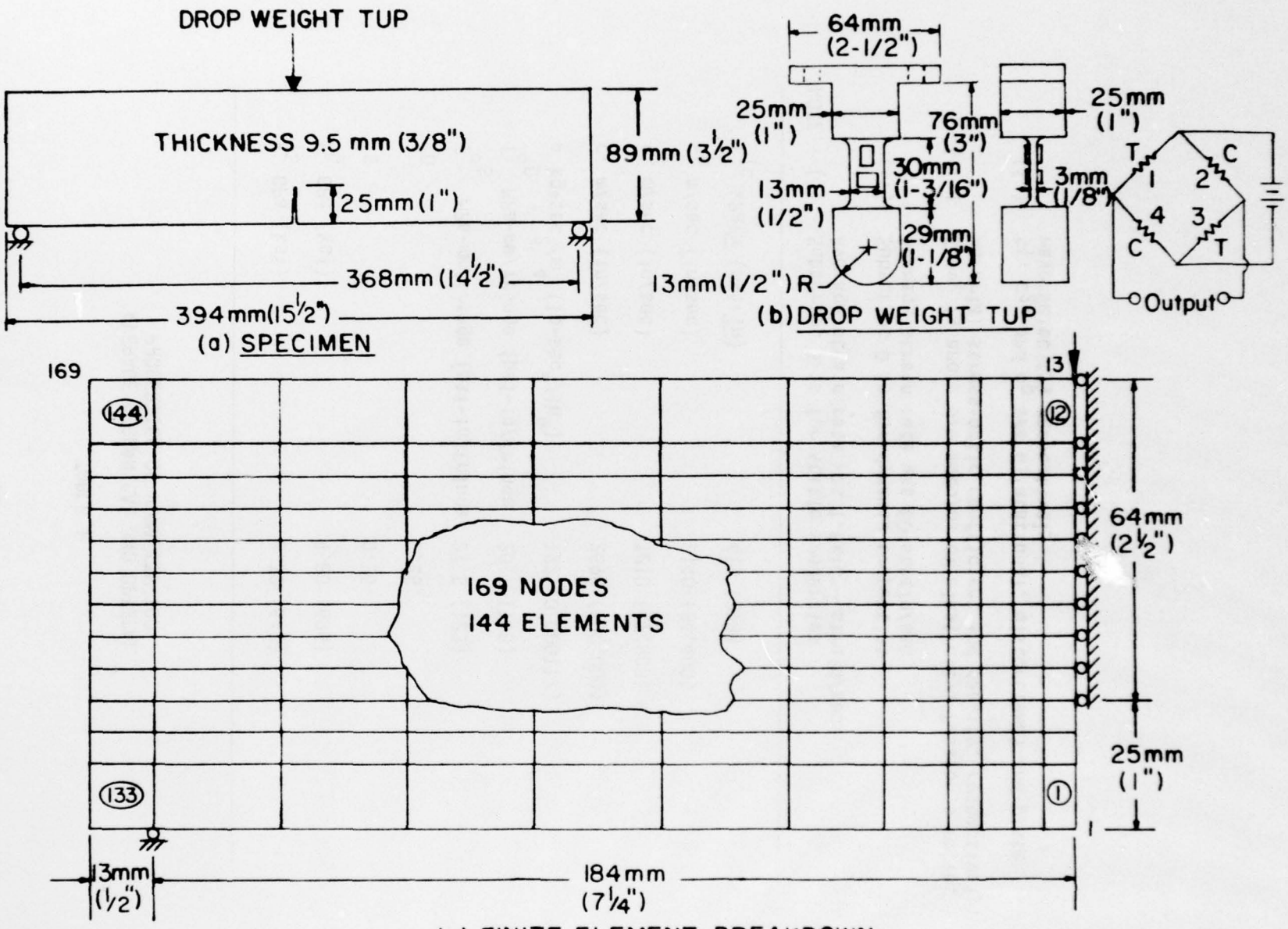

FIGURE 1. DYNAMIC TEAR TEST (DTT) SPECIMEN

(a) 5TH FRAME 190 μ SECONDS

(b) 7 TH FRAME 270 μ SECONDS

FIGURE 2. TYPICAL DYNAMIC PHOTOELASTIC PATTERNS IN HOMALITE-100 DTT SPECIMEN NO. S100976-1-H.

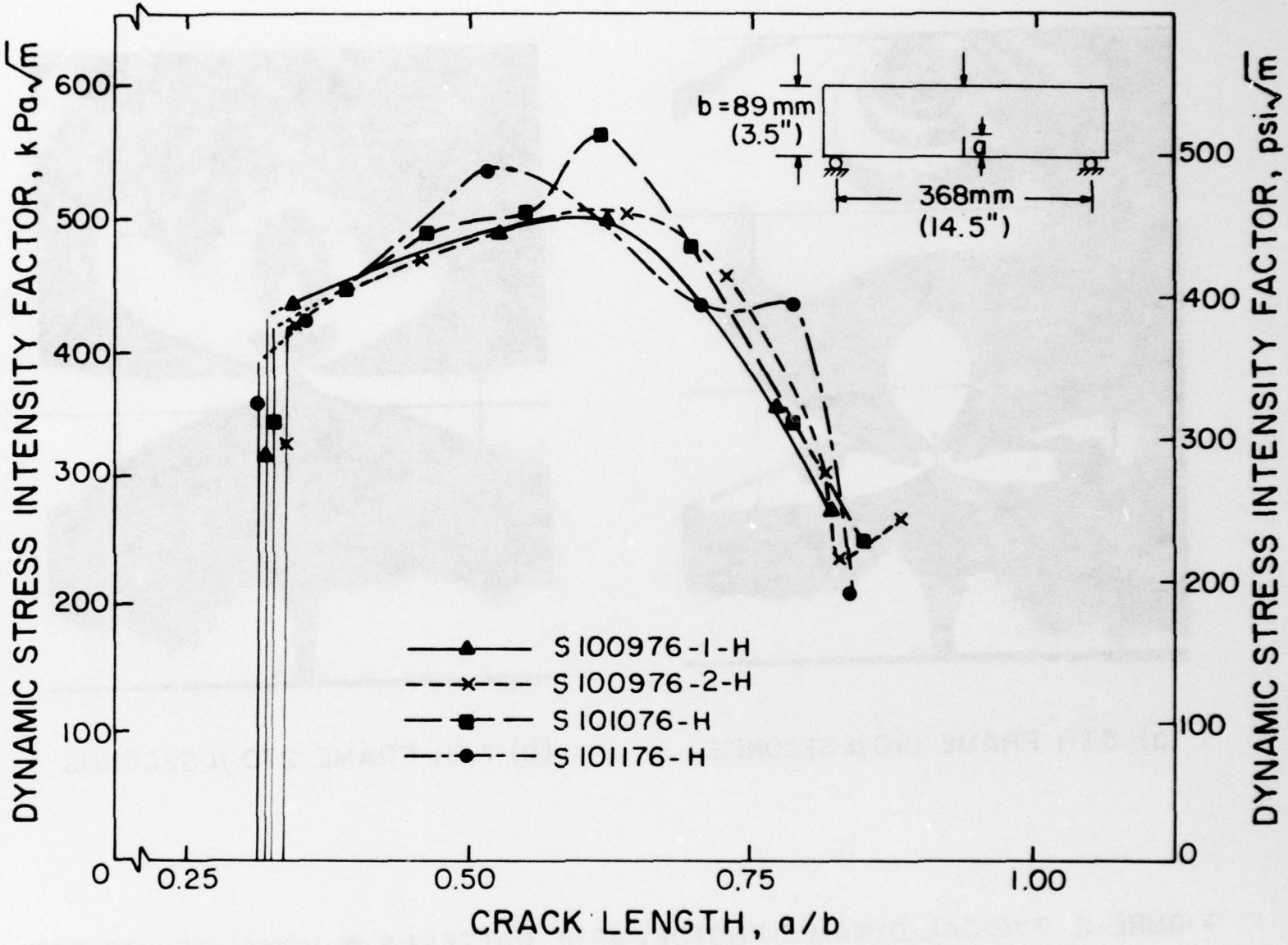

FIGURE 3. DYNAMIC STRESS INTENSITY FACTOR OF FOUR DDT SPECIMENS (HOMALITE-100).

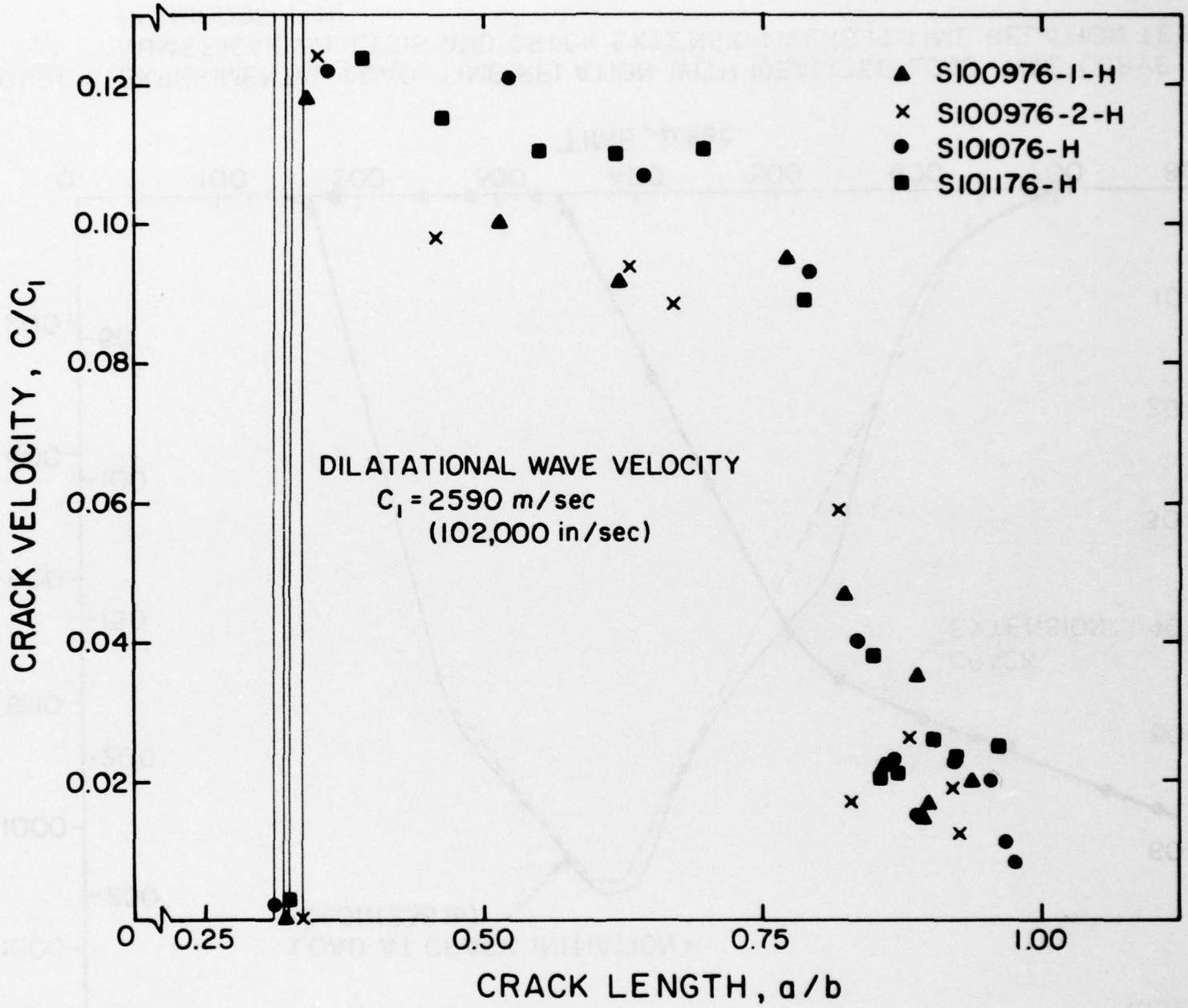

FIGURE 4. CRACK VELOCITIES OF FOUR DTT SPECIMENS (HOMALITE-100).

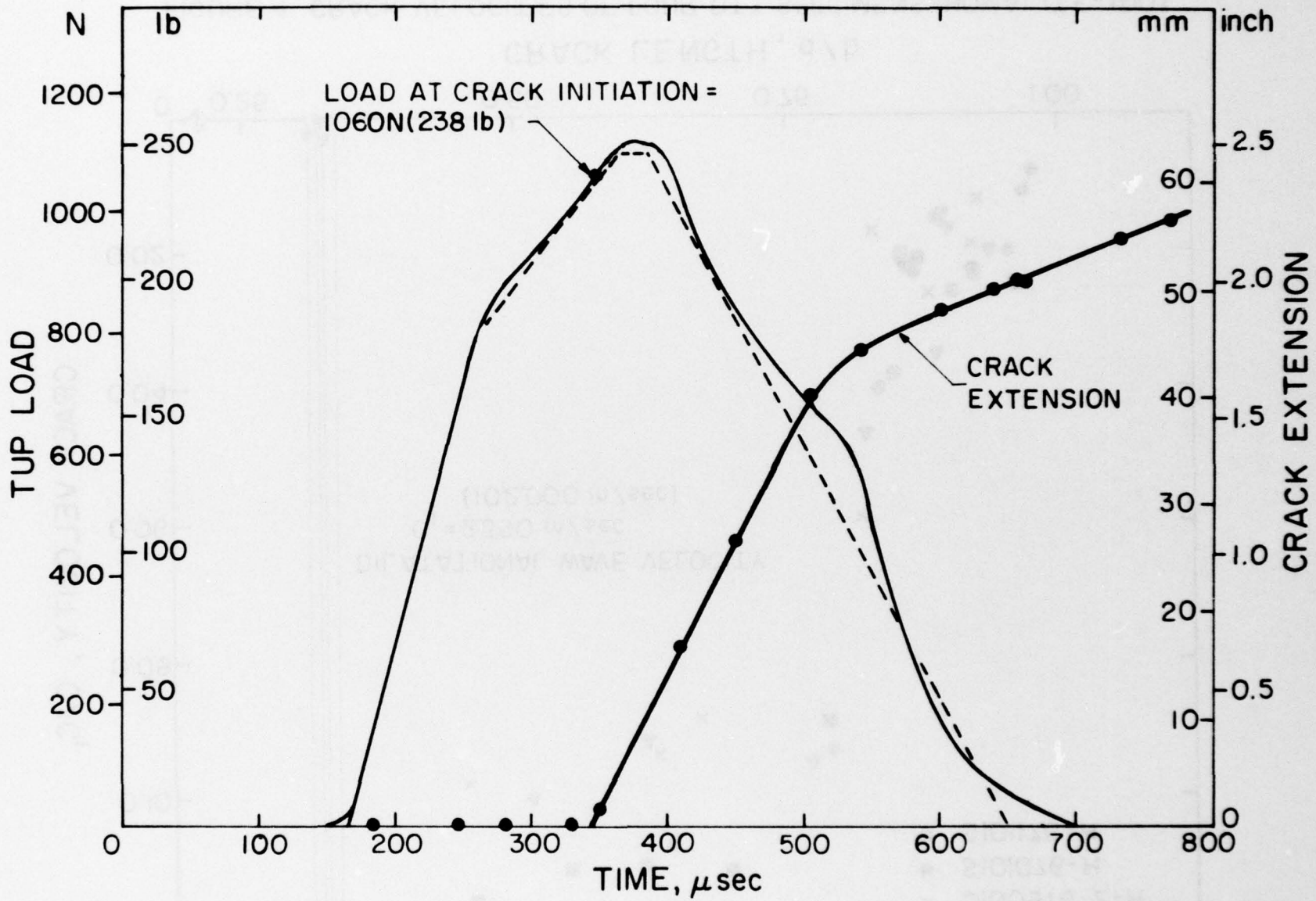

FIGURE 5. EXPERIMENTAL LOAD-TIME RELATION WITH IDEALIZED LOAD-TIME CURVE FOR NUMERICAL ANALYSIS AND CRACK EXTENSION VERSUS TIME RELATION TEST NO. S10096-1-H.

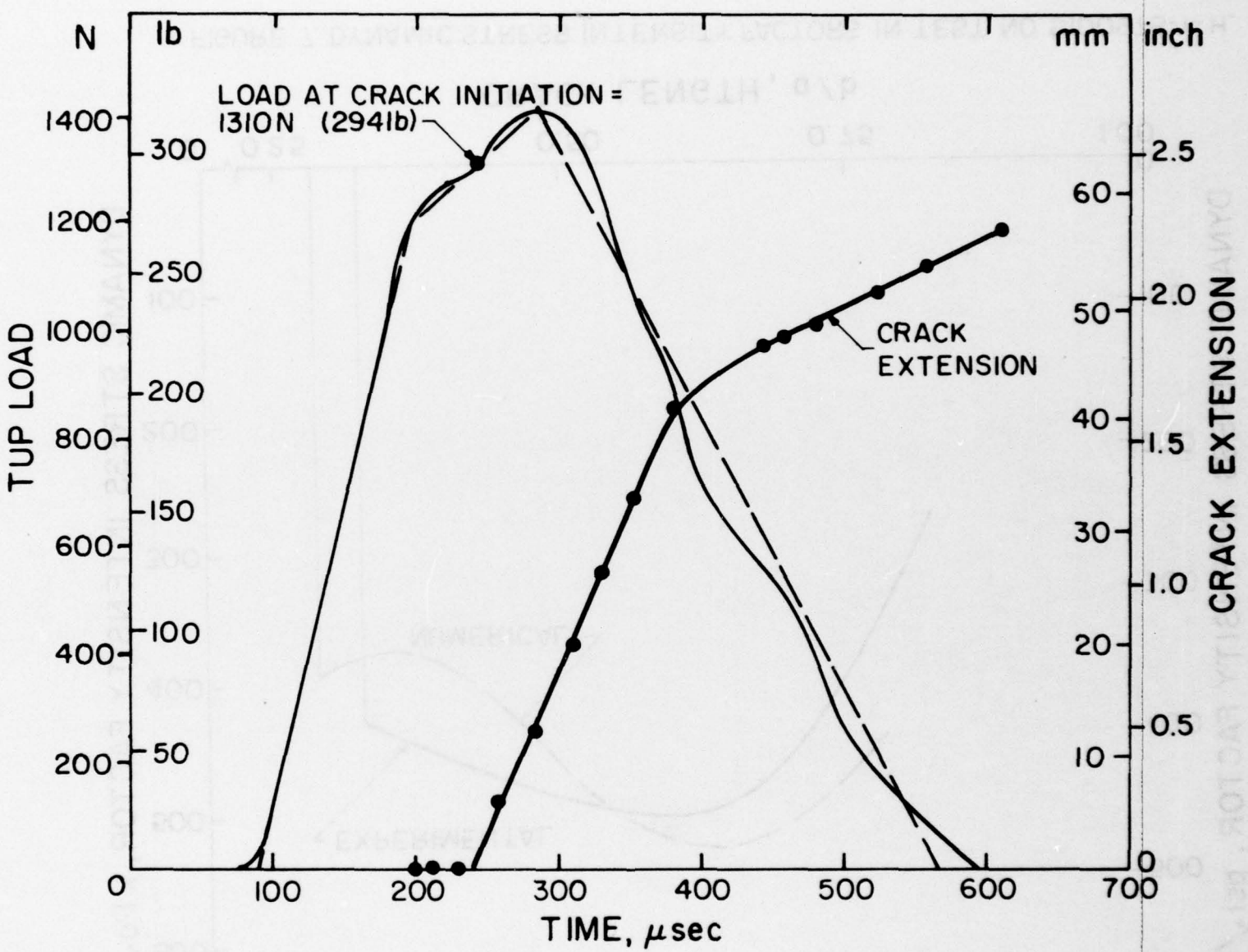

FIGURE 6. EXPERIMENTAL LOAD-TIME HISTORY WITH IDEALIZED LOAD-TIME CURVE FOR NUMERICAL ANALYSIS AND CRACK EXTENSION VERSUS TIME RELATION. TEST NO. S101176-H.

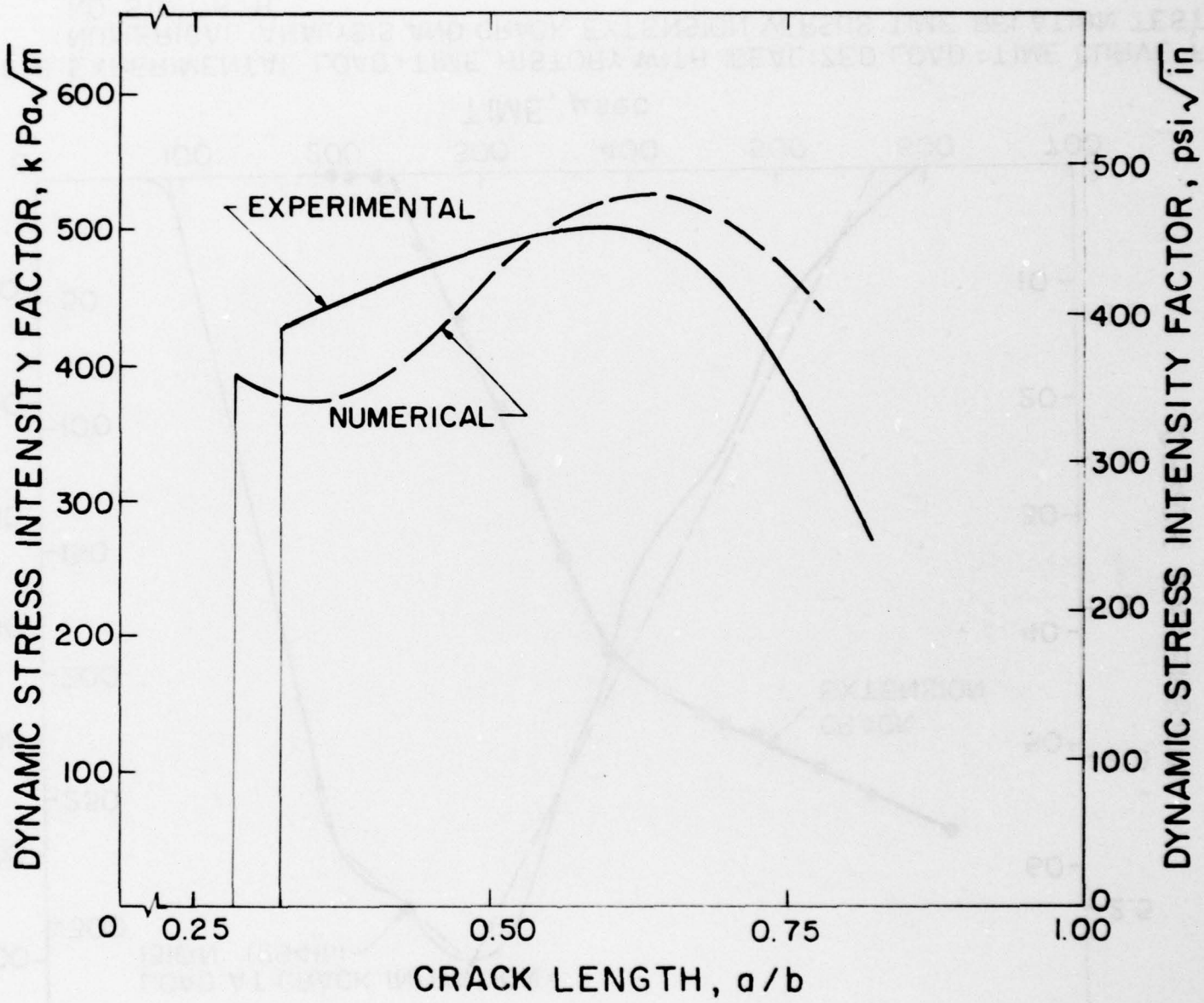

FIGURE 7. DYNAMIC STRESS INTENSITY FACTORS IN TEST NO. S100976-1-H.

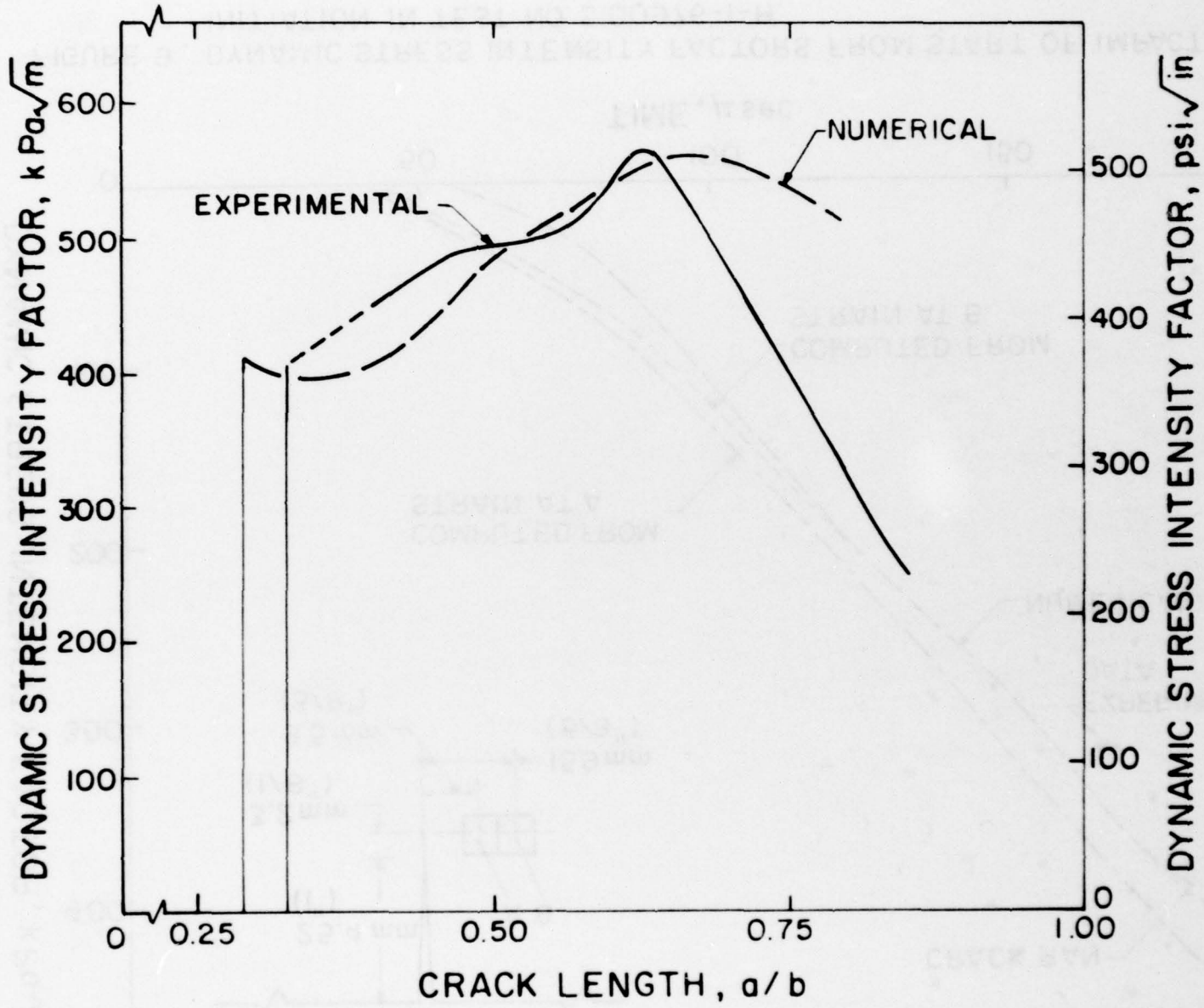

FIGURE 8. DYNAMIC STRESS INTENSITY FACTORS IN TEST NO. SIO1176-H.

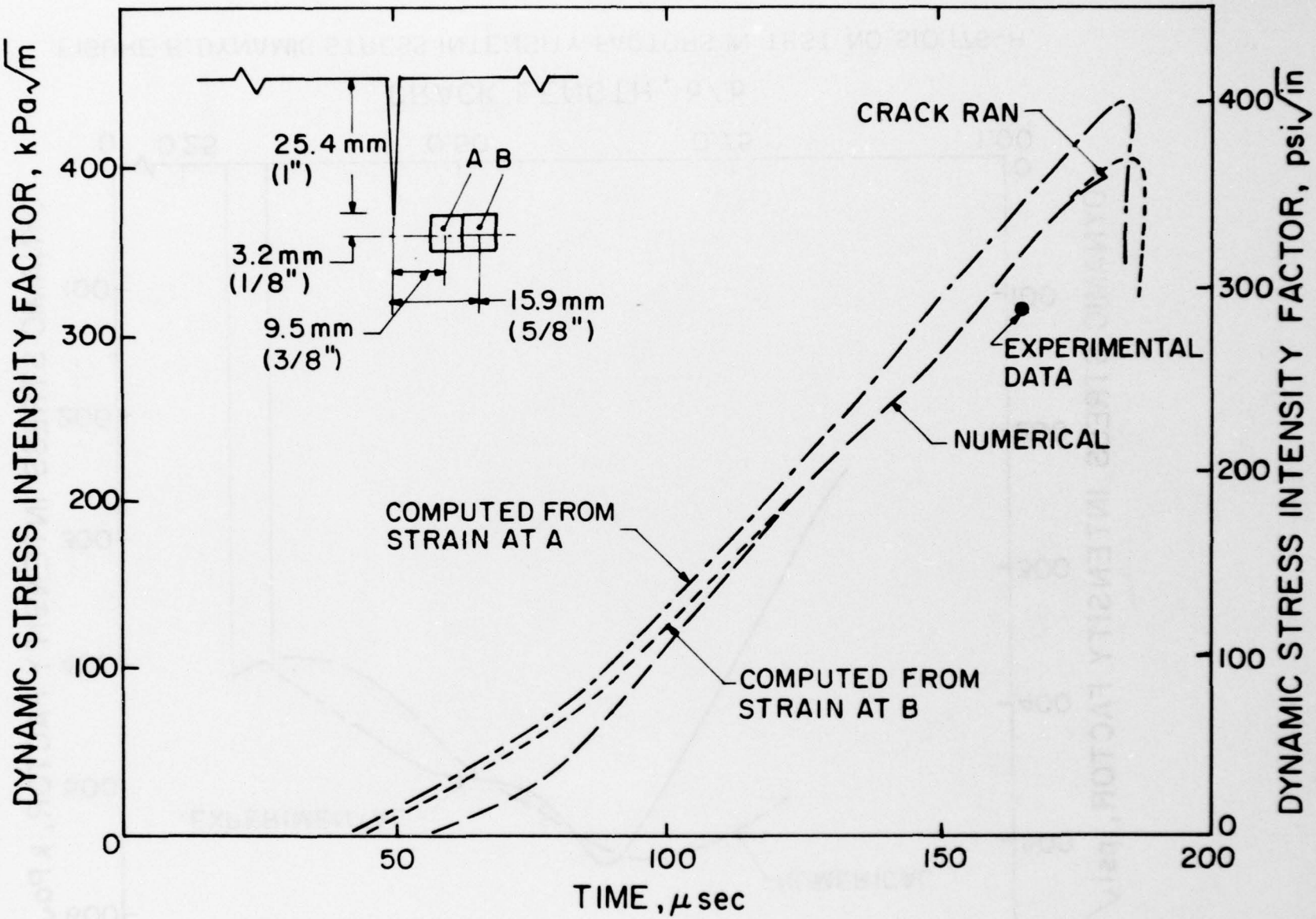

FIGURE 9. DYNAMIC STRESS INTENSITY FACTORS FROM START OF IMPACT TO CRACK INITIATION IN TEST NO. S100976-1-H.

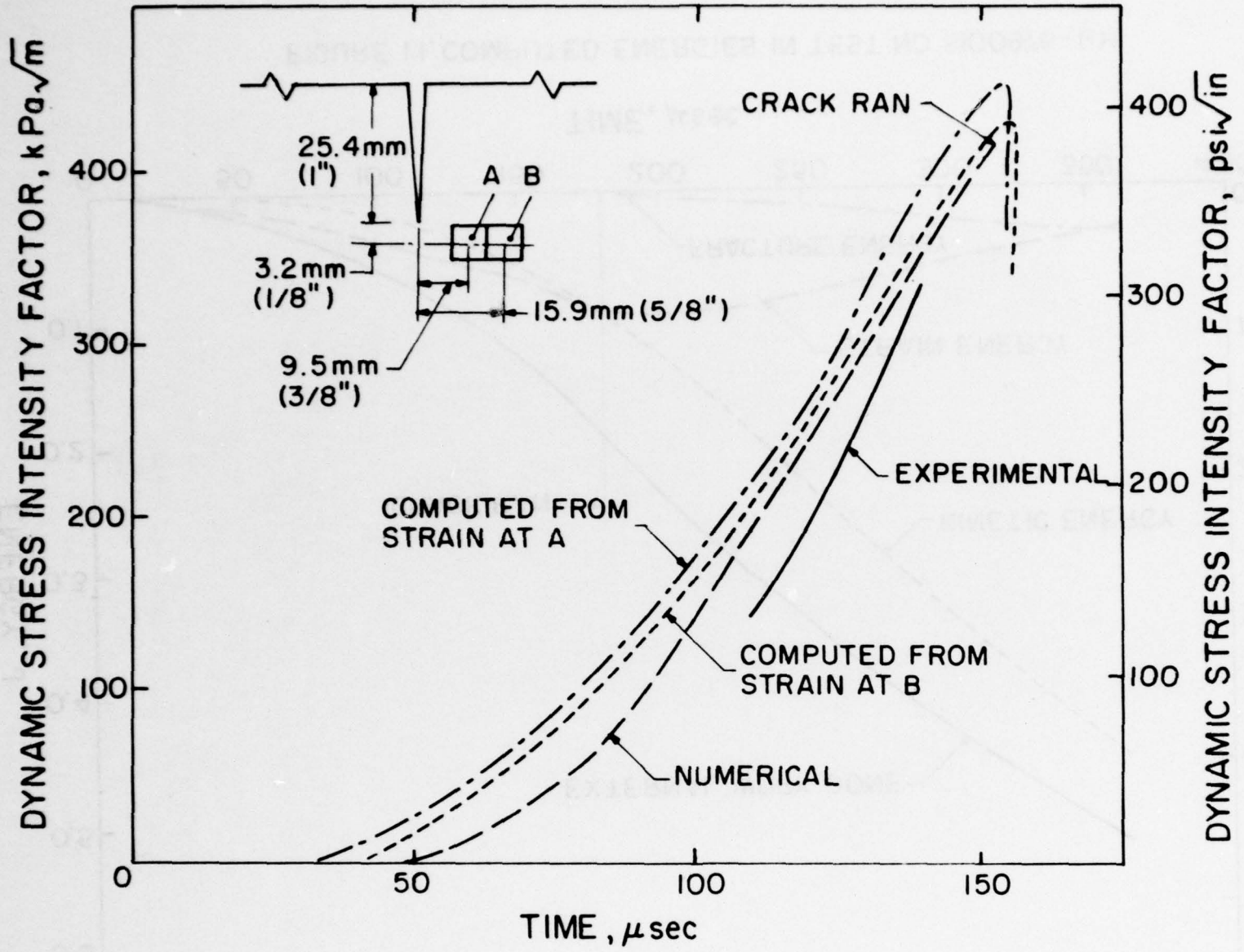

FIGURE 10. DYNAMIC STRESS INTENSITY FACTORS FROM START OF IMPACT TO CRACK INITIATION IN TEST NO. S101176-H.

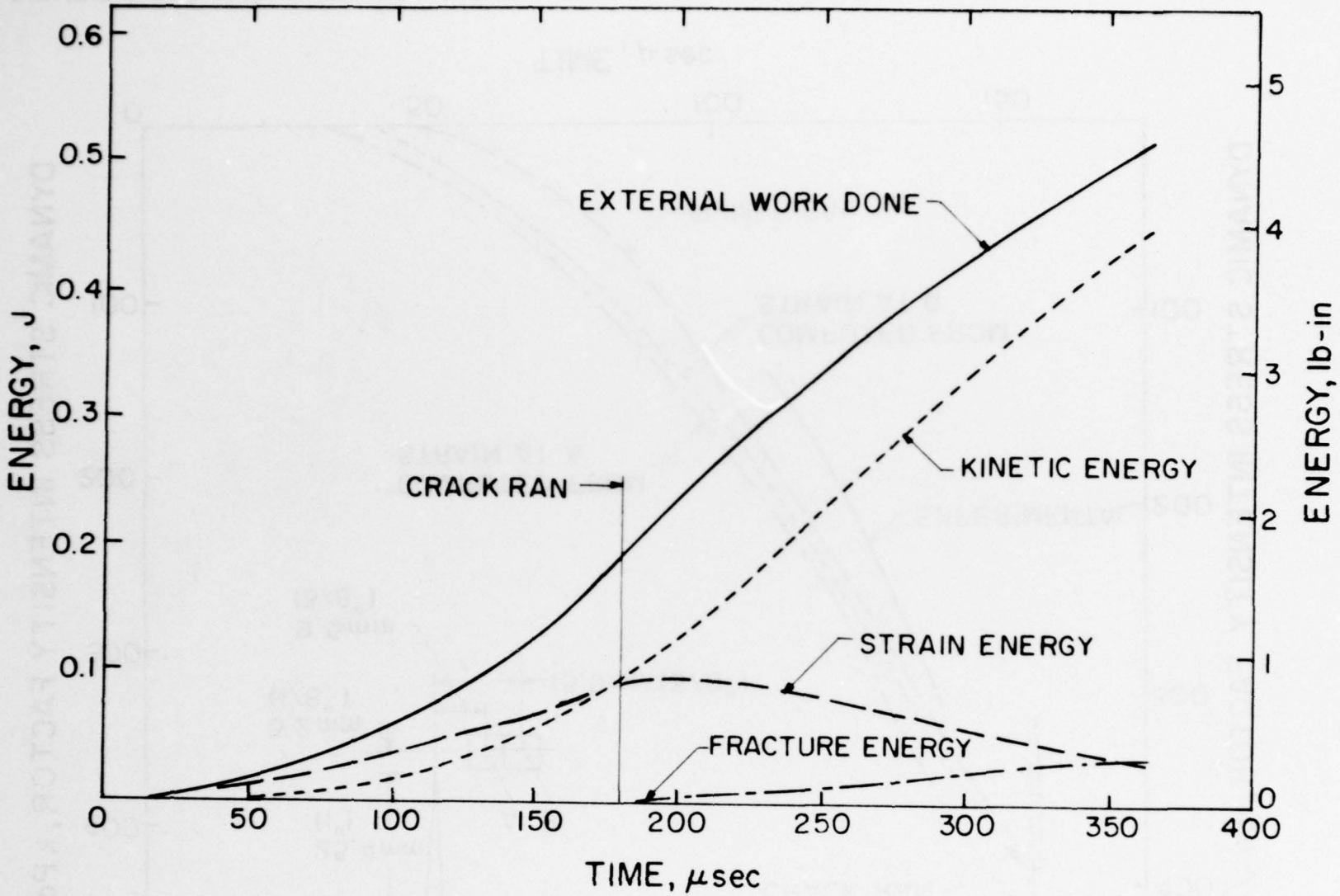

FIGURE 11. COMPUTED ENERGIES IN TEST NO. S100976-1-H

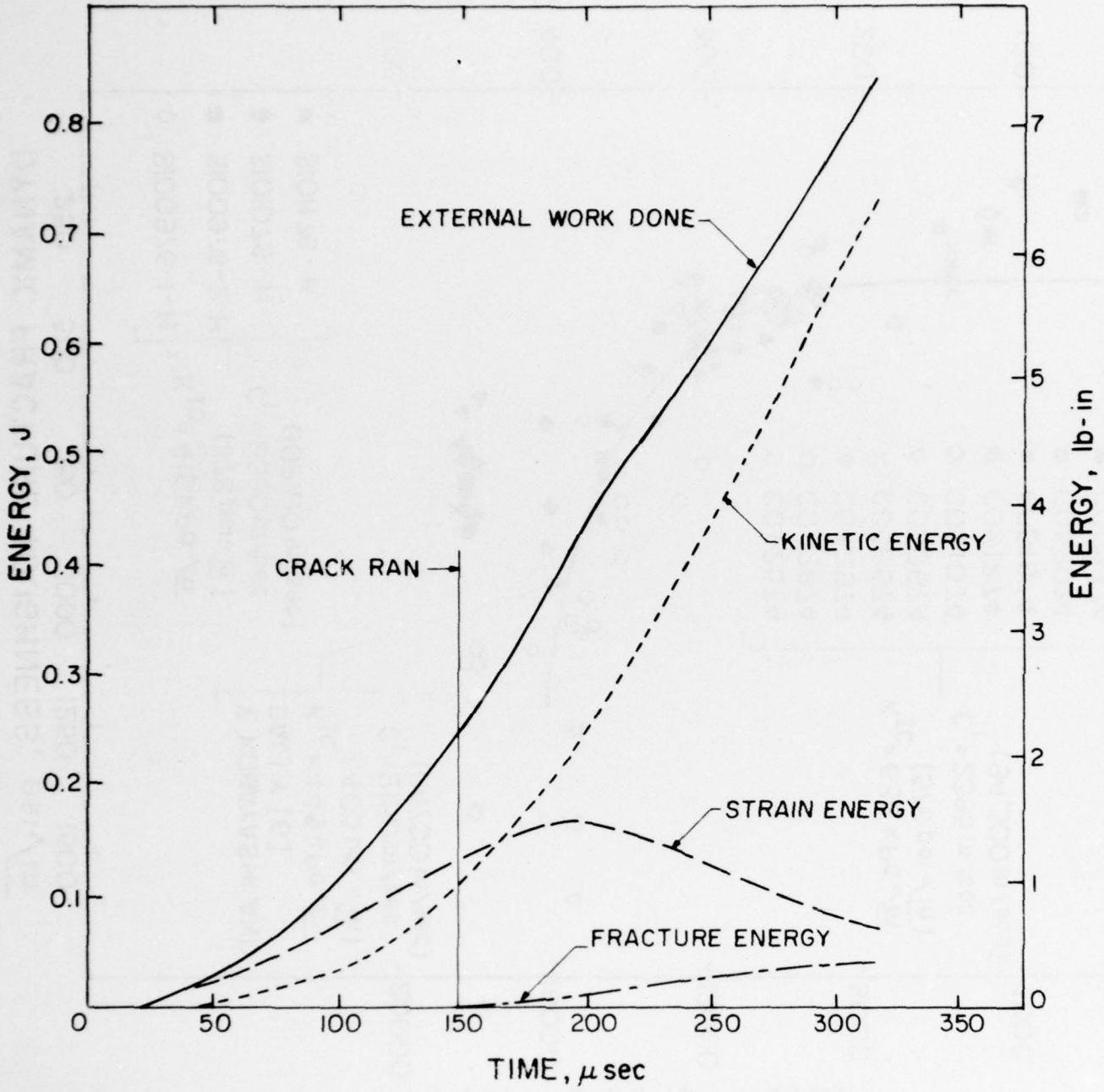

FIGURE 12. COMPUTED ENERGIES IN TEST NO. S1011176-H.

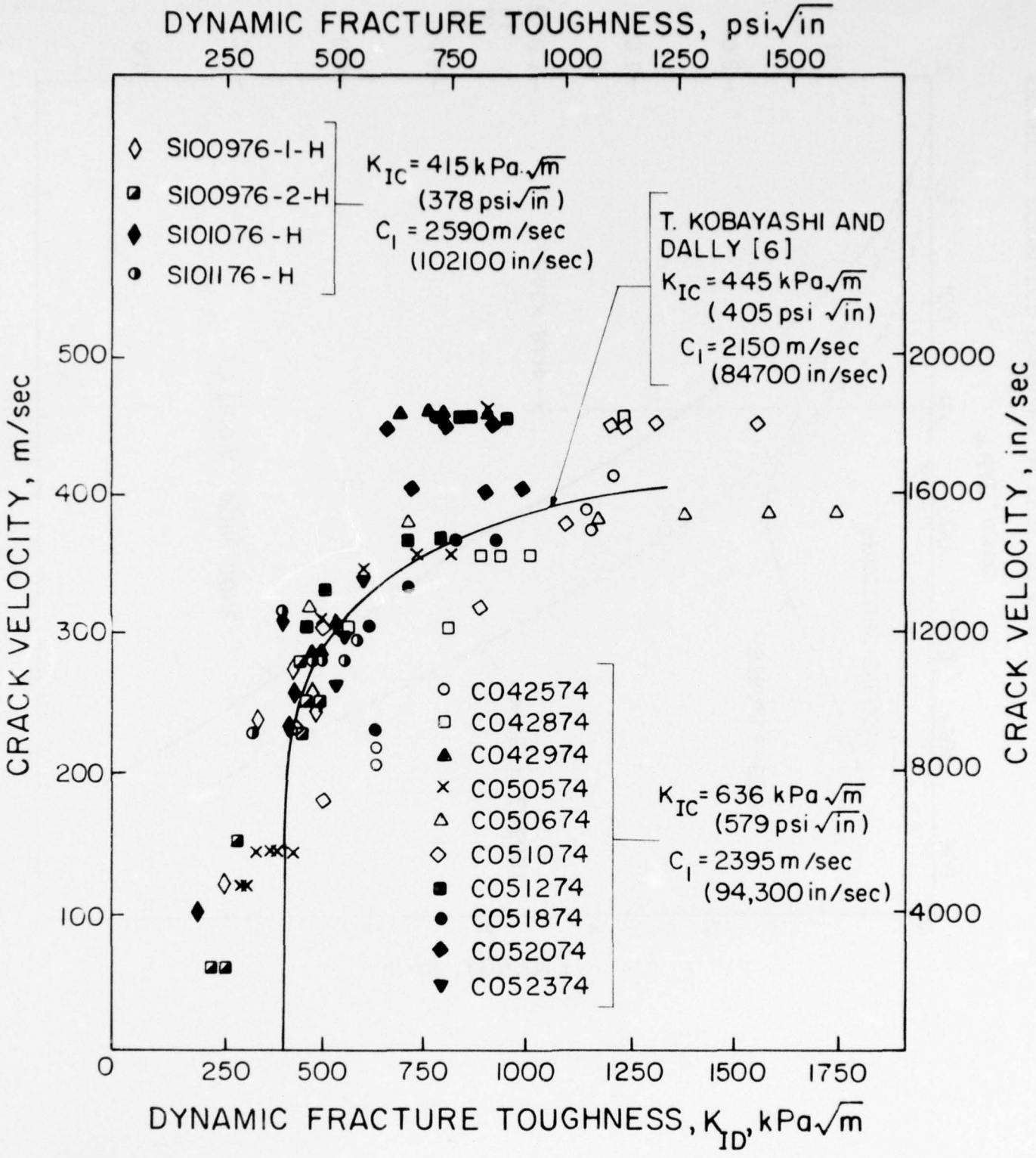

FIGURE 13. CRACK VELOCITY VERSUS DYNAMIC FRACTURE TOUGHNESS RELATIONS FOR HOMALITE-100

PART 1 - GOVERNMENT

Administrative and Liaison Activities

Office of Naval Research
Department of the Navy
Arlington, VA 22217
Attn: Code 474 (2
471
200

Director
Office of Naval Research Branch Office
495 Summer Street
Boston, MA 02210

Director
Office of Naval Research Branch Office
536 South Clark Street
Chicago, IL 60605

Director
Office of Naval Research
New York Area Office
715 Broadway - 5th Floor
New York, NY 10003

Director
Office of Naval Research Branch Office
1030 East Green Street
Pasadena, CA 91106

Director
Office of Naval Research
San Francisco Area Office
One Hallidie Plaza, Suite 601
San Francisco, CA 94102

Naval Research Laboratory (6)
Code 2627
Washington, D.C. 20375

Defense Documentation Center (12)
Cameron Station
Alexandria, VA 22314

NAVY

Naval Research Laboratory
Washington, D.C. 20375
Attn: Code 8400
8410
8430
8440
6300
6390
6380

Undersea Explosion Research Division
Naval Ship Research & Dev. Center
Norfolk Naval Shipyard
Portsmouth, VA 23709
Attn: Dr. E. Palmer, Code 177

Navy (Continued)

David W. Taylor Naval Ship Research
and Development Center
Annapolis, MD 21402
Attn: Code 2740
28
281

U.S. Naval Weapons Center
China Lake, CA 93555
Attn: Code 4062
4520

Commanding Office
U.S. Naval Civil Engineering Laboratory
Code L31
Port Hueneme, CA 93041

Naval Surface Weapons Center
White Oak
Silver Spring, MD 20910
Attn: Code WR-10
WA-20

Technical Director
Naval Ocean Systems Center
San Diego, CA 92152

Supervisor of Shipbuilding
U.S. Navy
Newport News, VA 23607

U.S. Navy Underwater Sound Reference Division
Naval Research Laboratory
P.O. Box 8337
Orlando, FL 32806

Chief of Naval Operations
Department of the Navy
Washington, DC 20350
Attn: Code OP-098

Strategic Systems Project Office
Department of the Navy
Washington, DC 20376
Attn: NSP-200

Naval Air Systems Command
Department of the Navy
Washington, DC 20361
Attn: Code 5302 (Aerospace & Structures)
604 (Technical Library)
320B (Structures)

Naval Air Development Center
Director, Aerospace Mechanics
Warminster, PA 18974

U.S. Naval Academy
Engineering Department
Annapolis, MD 21402

NASA (Continued)

Scientific & Technical Information Facility
NASA Representative (S-AK/DL)
P.O. Box 5700
Bethesda, MD 20014

Other Government Activities

Commandant
Chief, Testing & Development Division
U.S. Coast Guard
1300 E Street, NW
Washington, DC 20226

Technical Director
Marine Corps Development and
Education Command
Quantico, VA 22134

Director
National Bureau of Standards
Washington, DC 20034
Attn: Mr. B.L. Wilson, EM 219

Dr. M. Gaus
National Science Foundation
Environmental Research Division
Washington, DC 20550

Library of Congress
Science and Technology Division
Washington, DC 20540

Director
Defense Nuclear Agency
Washington, DC 20305
Attn: SPSS

Director Defense Research & Engineering
Technical Library
Room 3C128
The Pentagon
Washington, DC 20301

Mr. Jerome Persh
Staff Specialist for Materials
and Structures
ODDR&E, The Pentagon
Room 3D1089
Washington, DC 20301

Chief, Airframe & Equipment Branch
FS-120
Office of Flight Standards
Federal Aviation Agency
Washington, DC 20553

Chief, Research and Development
Maritime Administration
Washington, DC 20235

Picatinny Arsenal
Plastics Technical Evaluation Center
Attn: Technical Information Center
Dover, NJ 07801

Other Government Activities (Continued)

Deputy Chief, Offic of Ship Construction
Maritime Administration
Washington, DC 20235
Attn: Mr. U.L. Russo

National Academy of Sciences
National Research Council
Ship Hull Research Committee
2101 Constitution Avenue
Washington, DC 20418
Attn: Mr. A.R. Lytle

National Science Foundation
Engineering Mechanics Section
Division of Engineering
Washington, DC 20550

Navy (Continued)

Naval Facilities Engineering Command
200 Stovall Street
Alexandria, VA 22332
Attn: Code 03 (Research & Development)
048
045
14114 (Technical Library)

Naval Sea Systems Command
Department of the Navy
Washington, DC 20362
Attn: Code 03 (Research & Technology)
037 (Ship Silencing Division)
035 (Mechanics & Materials)

Naval Ship Engineering Center
Department of the Navy
Washington, DC 20362
Attn: Code 6105G
6114
6120D
6128
6129

Commanding Officer and Director
David W. Taylor Naval Ship Research
and Development Center
Bethesda, MD 20034
Attn: Code 042
17
172
173
174
1800
1102.1
1900
1901
1945
1960
1962

Naval Underwater Systems Center
Newport, RI 02840
Attn: Dr. R. Trainor

Naval Surface Weapons Center
Dahlgren Laboratory
Dahlgren, VA 22448
Attn: Code DG-20
DG-30

Technical Director
Mare Island Naval Shipyard
Vallejo, CA 94592

Army

Commanding Officer (2)
U.S. Army Research Office
P.O. Box 12211
Research Triangle Park, NC 27709
Attn: Mr. J.J. Murray, CRD-AA-IP

Army (Continued)

Watervliet Arsenal
MAGGS Research Center
Watervliet, NY 12189
Attn: Director of Research

U.S. Army Materials and Mechanics
Research Center
Watertown, MA 02172
Attn: Dr. R. Shea, DRXMR-T

U.S. Army Missile Research & Dev. Center
Redstone Scientific Information Center
Chief, Document Section
Redstone Arsenal, AL 35809

Army Research and Development Center
Fort Belvoir, VA 22060

Air Force

Commander WADD
Wright-Patterson Air Force Base
Dayton, OH 45433
Attn: Code WWRMDD
AFFDL (FDDS)
Structures Division
AFLC (MCEEA)

Chief, Applied Mechanics Group
U.S. Air Force Institute of Technology
Wright-Patterson Air Force Base
Dayton, OH 45433

Chief, Civil Engineering Branch
WLRC, Research Division
Air Force Weapons Laboratory
Kirtland Air Force Base
Albuquerque, NM 87117

Air Force Office of Scientific Research
Bolling Air Force Base
Washington, DC 20332
Attn: Mechanics Division

Department of the Air Force
Air University Library
Maxwell Air Force Base
Montgomery, AL 36112

NASA

National Aeronautics & Space Administration
Structures Research Division
Langley Research Center
Langley Station
Hampton, VA 23365

National Aeronautics & Space Administration
Associate Administrator for Advanced
Research and Technology
Washington, D.C 20546

PART 2 - CONTRACTORS AND OTHER TECHNICAL COLLABORATORS

Universities

Dr.J. Tinsley Oden
University of Texas at Austin
345 Engineering Science Building
Austin, TX 78712

Professor Julius Miklowitz
California Institute of Technology
Div. of Engineering & Applied Sciences
Pasadena, CA 91109

Dr. Harold Liebowitz, Dean
School of Engineering & Applied Science
George Washington University
Washington, DC 20052

Professor Eli Sternberg
California Institute of Technology
Div. of Engineering & Applied Science
Pasadena, CA 91109

Professor Paul M. Naghdi
University of California
Department of Mechanical Engineering
Berkeley, CA 94720

Professor P.S. Symonds
Brown University
Division of Engineering
Providence, RI 02912

Professor A.J. Durelli
Oakland University
School of Engineering
Rochester, MI 48063

Professor F.L. DiMaggio
Columbia University
Department of Civil Engineering
New York, NY 10027

Professor Norman Jones
Massachusetts Institute of Technology
Department of Ocean Engineering
Cambridge, MA 02139

Professor E.J. Skudrzyk
Pennsylvania State University
Applied Research Laboratory
Department of Physics
State College, PA 16801

Professor J. Kempner
Polytechnic Institute of New York
Dept. of Aerospace Engrg. & Applied Mech.
333 Jay Street
Brooklyn, NY 11201

Professor J. Klosner
Polytechnic Institute of New York
Dept. of Aerospace Engrg. & Applied Mechanics
333 Jay Street
Brooklyn, NY 11201

Professor R.A. Schapery
Texas A&M University
Department of Civil Engineering
College Station, TX 77843

Professor Walter D. Pilkey
University of Virginia
Research Laboratories for the Engineering
Sciences
School of Engineering and Applied Sciences
Charlottesville, VA 22901

Professor K.D. Willmert
Clarkson College of Technology
Department of Mechanical Engineering
Potsdam, NY 13676

Dr. H.G. Schaeffer
University of Maryland
Aerospace Engineering Department
College Park, MD 20742

Dr. Walter E. Haisler
Texas A&M University
Aerospace Engineering Department
College Station, TX 77843

Dr. B.S. Berger
University of Maryland
Department of Mechanical Engineering
College Park, MD 20742

Dr. L.A. Schmit
University of California
School of Engineering & Applied Science
Los Angeles, CA 90024

Dr. Hussein A. Kamel
University of Arizona
Dept. of Aerospace & Mechanical Engineering
Tucson, AZ 85721

Dr. S.J. Fenves
Carnegie-Mellon University
Department of Civil Engineering
Schenley Park
Pittsburgh, PA 15213

Dr. Ronald L. Huston
Dept. of Engineering Analysis
University of Cincinnati
Cincinnati, OH 45221

Universities (Continued)

Professor G.C.M. Sih
Lehigh University
Institute of Fracture and
Solid Mechanics
Bethlehem, PA 18015

Professor Albert S. Kobayashi
University of Washington
Department of Mechanical Engineering
Seattle, WA 98195

Professor Daniel Frederick
Virginia Polytechnic Institute and
State University
Dept. of Engineering Mechanics
Blacksburg, VA 24061

Professor A.C. Eringen
Dept. of Aerospace & Mech. Sciences
Princeton University
Princeton, NJ 08540

Professor E.H. Lee
Stanford University
Div. of Engineering Mechanics
Stanford, CA 94305

Professor Albert I. King
Wayne State University
Biomechanics Research Center
Detroit, MI 48202

Dr. V.R. Hodgson
Wayne State University
School of Medicine
Detroit, MI 48202

Dean B.A. Boley
Northwestern University
Department of Civil Engineering
Evanston, IL 60201

Professor P.G. Hodge, Jr.
University of Minnesota
Dept. of Aerospace Engineering
and Mechanics
Minneapolis, MN 55455

Dr. D.C. Drucker
University of Illinois
Dean of Engineering
Urbana, IL 61801

Professor N.M. Newmark
University of Illinois
Dept. of Civil Engineering
Urbana, IL 61803

Professor E. Reissner
University of California, San Diego
Dept. of Applied Mechanics
La Jolla, CA 92037

Professor William A. Nash
University of Massachusetts
Dept. of Mechanics & Aerospace Engineering
Amherst, MA 01002

Professor G. Herrmann
Stanford University
Department of Applied Mechanics
Stanford, CA 94305

Professor J.D. Achenbach
Northwestern University
Department of Civil Engineering
Evanston, IL 60201

Professor G.R. Irwin
University of Maryland
Dept. of Mechanical Engineering
College Park, MD 20742

Professor S.B. Dong
University of California
Department of Mechanics
Los Angeles, CA 90024

Professor Burt Paul
University of Pennsylvania
Towne School of Civil and
Mechanical Engineering
Philadelphia, PA 19104

Professor H.W. Liu
Syracuse University
Dept. of Chemical Engineering & Metallurgy
Syracuse, NY 13210

Professor S. Bodner
Technion R&D Foundation
Haifa, Israel

Professor Werner Goldsmith
University of California
Dept. of Mechanical Engineering
Berkeley, CA 94720

Professor R.S. Rivlin
Lehigh University
Center for the Application of Mathematics
Bethlehem, PA 18015

Professor F.A. Cozzarelli
State University of New York at Buffalo
Div. of Interdisciplinary Studies
Karr Parker Engineering Building
Chemistry Road
Buffalo, NY 14214

Professor Joseph L. Rose
Drexel University
Dept. of Mechanical Engineering & Mechanics
Philadelphia, PA 19104

Universities (Continued)

Professor Kent R. Wilson
University of California, San Diego
Department of Chemistry
La Jolla, CA 92093

Professor B.K. Donaldson
University of Maryland
Aerospace Engineering Department
College Park, MD 20742

Professor Joseph A. Clark
Catholic University of America
Dept. of Mechanical Engineering
Washington, DC 20064

Professor T.C. Huang
University of Wisconsin-Madison
Dept. of Engineering Mechanics
Madison, WI 53706

Dr. Samuel B. Batdorf
University of California
School of Engineering & Applied Science
Los Angeles, CA 90024

Industry and Research Institutes

U.S. Naval Postgraduate School
Library
Code 0384
Monterey, CA 93940

Webb Institute of Naval Architecture
Attn: Librarian
Crescent Beach Road, Glen Cove
Long Island, NY 11542

Unclassified

SECURITY CLASSIFICATION OF THIS PAGE (When Data Entered)

REPORT DOCUMENTATION PAGE		READ INSTRUCTIONS BEFORE COMPLETING FORM
1. REPORT NUMBER 31	2. GOVT ACCESSION NO.	3. RECIPIENT'S CATALOG NUMBER
4. TITLE (and Subtitle) Dynamic Photoelastic and Dynamic Finite Element Analyses of Dynamic Tear Test Specimens		5. TYPE OF REPORT & PERIOD COVERED Interim Report 6. PERFORMING ORG. REPORT NUMBER 31
7. AUTHOR(s) S. Mall, A.S. Kobayashi and Y. Urabe		8. CONTRACT OR GRANT NUMBER(s) N00014-76-C-0060 NR 064-478
9. PERFORMING ORGANIZATION NAME AND ADDRESS University of Washington Department of Mechanical Engineering Seattle, Washington 98195		10. PROGRAM ELEMENT, PROJECT, TASK AREA & WORK UNIT NUMBERS
11. CONTROLLING OFFICE NAME AND ADDRESS Office of Naval Research Arlington, Virginia		12. REPORT DATE January 1973 13. NUMBER OF PAGES 25
14. MONITORING AGENCY NAME & ADDRESS(if different from Controlling Office)		15. SECURITY CLASS. (of this report) Unclassified 15a. DECLASSIFICATION/DOWNGRADING SCHEDULE

16. DISTRIBUTION STATEMENT (of this Report)

Unlimited

17. DISTRIBUTION STATEMENT (of the abstract entered in Block 20, if different from Report)

18. SUPPLEMENTARY NOTES

19. KEY WORDS (Continue on reverse side if necessary and identify by block number)

Fracture Mechanics, Fracture Dynamics, Crack Propagation, Crack Arrest, Finite Element Analysis, Dynamic Photoelasticity

20. ABSTRACT (Continue on reverse side if necessary and identify by block number)

Dynamic photoelasticity and dynamic finite element methods were used to study the transient response of dynamic tear test (DTT) specimen of a brittle material Homalite-100. The dynamic stress intensity factors obtained from dynamic photoelasticity and dynamic finite element analysis were generally in excellent agreement with each other and showed that the NRL procedure of computing the dynamic fracture initiation thoughness from strain gage measurements near the crack tip was reasonably accurate. Dynamic fracture toughness versus crack velocity relations were also obtained.

DD FORM 1 JAN 73 1473 EDITION OF 1 NOV 65 IS OBSOLETE
S/N 0102-014-6601

Unclassified

SECURITY CLASSIFICATION OF THIS PAGE (When Data Entered)